arXiv:1304.3315v1 [cond-mat.supr-con] 11 Apr 2013

Carrier flow caused by radiative recombination process in superconductor-based light-emitting diode

Ryotaro Inoue,[1, 2, *] Hideaki Takayanagi,[3, 4, 2] Tatsushi Akazaki,[5, 2]
Kazunori Tanaka,[6, 2] Hirotaka Sasakura,[7, 2] and Ikuo Suemune[7, 2]

[1] *Research Center for Advanced Science and Technology,*
Univ. of Tokyo, Tokyo 153-8904, Japan.
[2] *CREST, Japan Science and Technology Agency, Kawaguchi 332-0012, Japan.*
[3] *Dept. of Applied Physics, Tokyo Univ. of Science, Tokyo 162-8601, Japan.*
[4] *MANA, National Inst. for Materials Science, Tsukuba 305-0044, Japan.*
[5] *NTT Basic Research Lab., Kanagawa 243-0198, Japan.*
[6] *Central Research Lab., Hamamatsu Photonics K.K., Hamamatsu 434-8601, Japan.*
[7] *Research Inst. for Electronic Science,*
Hokkaido Univ., Sapporo 060-8628, Japan.

(Dated: April 12, 2013)

Abstract

Transport properties of Josephson junction attached to superconductor-based light-emitting diode (superconductor-based LED) are investigated and quantitatively explained. In the gate-controlled region, we confirm the realization of new-type Josephson field effect transistor (JoFET), where the channel cross-sectional area of the junction is directly modulated. In the current-injected region, the energy relaxation process of generated photons in succession to the radiative recombination process causes the conversion of superconducting pairs to quasiparticles in the active layer. Using two-fluid model, we discuss the carrier flows between the active layer and the superconducting electrodes, which takes place for compensating the conversion.

Superconductor-based light-emitting diode (superconductor-based LED) is expected to be the key device in quantum information technology because of its possible *on-demand* generation of entangled photon pairs, which comes from the coherence of superconducting Cooper pairs. In addition to theoretical studies [1, 2], the radiative recombination process in superconductor-based LED has been studied by optical measurements, which reveal the enhanced oscillator strength [3], high quantum efficiency and radiative recombination time rapidly decreasing with temperature [4, 5]. The transport measurement, on the other hand, demonstrated the diffusion of superconducting pairs into the active layer by DC and AC Josephson effect, together with the monitoring of radiative recombination process, the sensitivity of which is several orders higher than that in optical measurement [4–6].

The structure of superconductor-based LED with one normal electrode at the p-type semiconductor side and two superconducting electrodes at the n-type semiconductor side can be considered as a superconductor-based three-terminal device, which has attracted research interests as Josephson Field Effect Transistor (JoFET) [7], modulation of superconducting critical current by normal carrier injection (including 0-π transition) [8, 9], cross Andreev reflection [10, 11] and so forth. In this letter, we quantitatively discuss the radiative recombination process in superconductor-based LED studied by the transport properties as a new-type superconductor-based three-terminal device.

Figure 1(a) shows the schematic cross-sectional view of superconductor-based LED, where p-type indium phosphide (p-InP) layer and n-type indium gallium arsenide (n-InGaAs) layer are stacked on p-InP substrate, and form a p-n junction heterostructure. When positive / negative voltage is applied to the gate electrode under the p-InP substrate, the p-n junction is biased forward / inversely. Two niobium (Nb) superconducting electrodes with a thickness of 800 Å are attached to the n-InGaAs layer, where superconducting pairs together with quasiparticles diffuse due to the proximity effect. Under the forward-biased condition, holes injected from the p-InP layer recombine with the superconducting pairs and quasiparticles in the n-InGaAs active layer. The resultant electroluminescence (EL) emission can be detected from the slit between the two Nb electrodes, the width of which is 150 nm. Figures 1(b) and 1(c) show EL spectrum and spectrally-integrated EL intensity as a function of injected current, which are measured in the sample with the same composition but with different slit width. It is found that the EL emission of $\sim$0.86 eV, which reflects the band structure of p-n junction, is obtained with the intensity roughly proportional to the injected current.

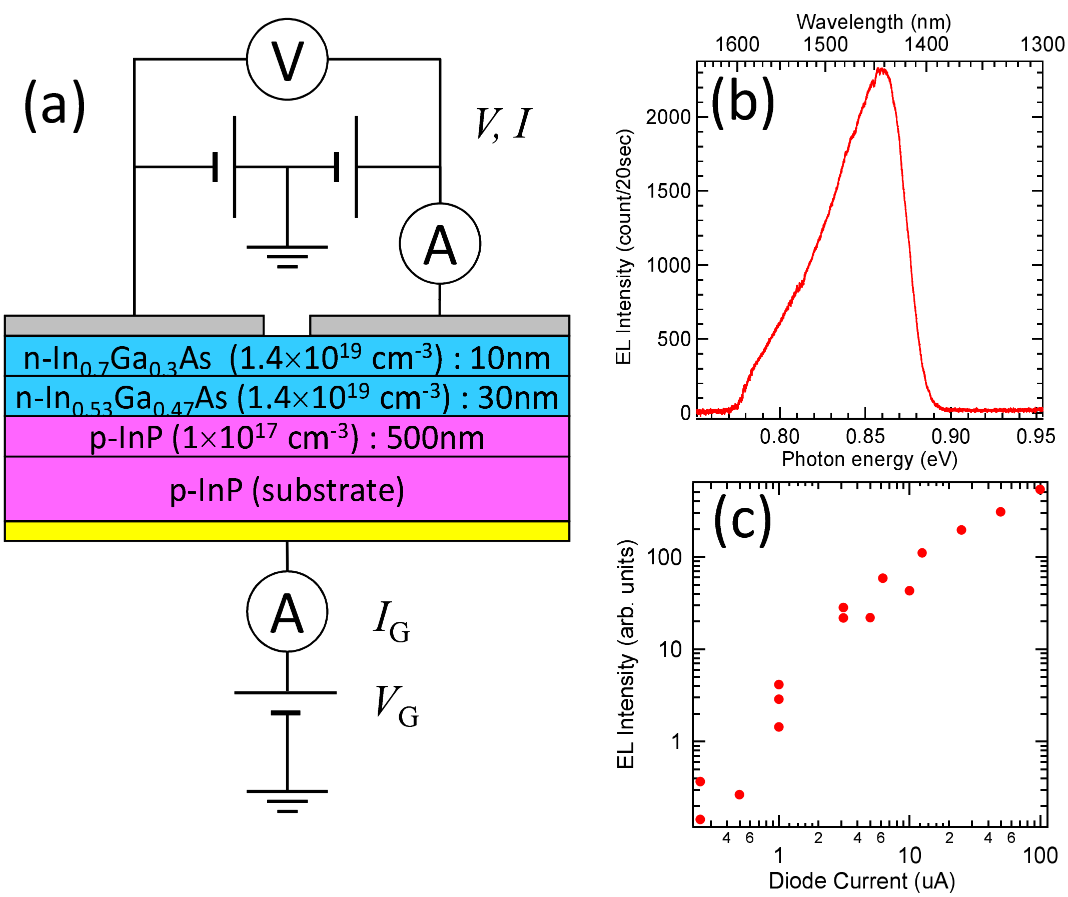

FIG. 1. (a) Schematic cross-sectional view of superconductor-based LED together with the measurement circuit. (b) EL spectrum of superconductor-based LED under the injection of 10 μA and (c) spectrally-integrated EL intensity as a function of injection. EL data are measured at 0.3 K, in the similar device with different gap between two Nb superconducting electrodes.

The two Nb superconducting electrodes together with the n-InGaAs layer between them form a superconductor - semiconductor - superconductor Josephson junction structure. We investigated the Josephson junction characteristics with changing the gate voltage (V_G) and / or the injected current (I_G), at a temperature of 30 mK using a dilution refrigerator. The measurement circuit is also shown in Fig. 1(a). In the measurement of Josephson junction characteristics, we biased the junction in such a way that the averaged electric potential of the two Nb electrodes is kept at 0 V. Therefore, when the hole current is injected from the gate electrode, the corresponding current is extracted via both of two Nb electrodes. From the preliminary Hall measurement at 0.3 K, the carrier density and carrier mobility in the n-InGaAs layer are obtained as 1.4×10^{19} cm^{-3} and 1.6×10^{3} cm^{2}/Vs, respectively. Since the mean free path (ℓ) and the thermal coherence length (ξ_N) at 30 mK are estimated to be ~75 nm and ~1.25 μm, the Josephson junction can be considered as *dirty* and *short* ($\ell < L < \xi_N$).

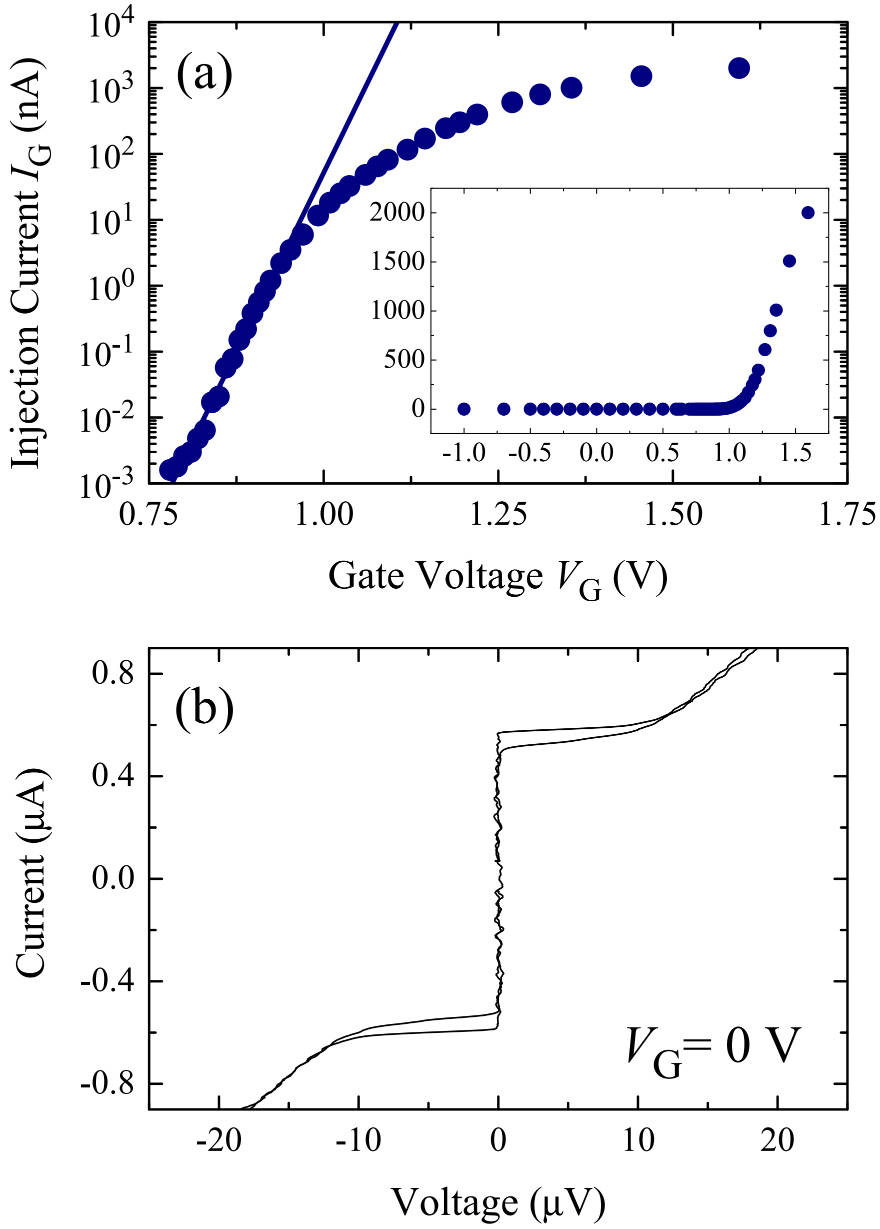

FIG. 2. (a)p-n junction characteristics of superconductor-based LED. The main panel and the inset are semilog plot and linear plot, respectively. (b) Josephson junction characteristics of superconductor-based LED with the gate voltage (V_G) of 0 V.

Figure 2(a) shows the injected hole current (I_G) as a function of applied gate voltage (V_G). Steady current injection of $I_G = 1.6$ pA starts at $V_G = 0.78$ V. Although we obtain the typical p-n junction diode characteristics $I_G \sim \exp(eV_G/\eta k_B T)$ with a non-ideal coefficient $\eta \sim 7.7 \times 10^3$, the tendency of saturation can be observed at $I_G \gtrsim 10$ nA. The hysteretic current - voltage characteristics of the Josephson junction with $V_G = 0$ V is shown in Fig. 2(b). The superconducting critical current (I_c) and the normal resistance (R_n) defined in sufficiently large current range, are 0.58 μA and 380 Ω, respectively. With the increasing temperature upto 160 mK, I_c declines as $\sim T^{-1/4}$ while R_n takes a constant value. When we apply the gate voltage (V_G), both I_c and R_n are found to be changed as shown in Fig. 3(a), which we will discuss in detail.

In the gate-controlled region of V_G <0.78 V, where we do not observe steady current injection, a depletion layer remains at the boundary of p-InP - n-InGaAs heterostructure. In this region, we succeeded in quantitative explaining of the behavior of Josephson junction characteristics (I_c and R_n) by the modulation of depletion layer thickness. This is a new-type JoFET, where the channel cross-sectional area is directly modulated by the gate voltage while the carrier density in semiconductor (normal metal) is modulated in conventional JoFET [7]. The critical current (I_c) and the normal resistance (R_n) can be written as follows in *dirty* and *short* junctions using the effective mass (m^*) and mobility (μ) of carrier:

$$\begin{aligned} I_c &= \frac{e n_p \hbar}{m^*} \frac{W(H - x(V_G))}{L}, \\ R_n &= R_0 + \frac{1}{e n_q \mu} \frac{L}{W(H - x(V_G))}. \end{aligned} \tag{1}$$

Here, L (150 nm), H (40 nm) and W are the length, thickness and width of the junction, and n_q and n_p are the quasiparticle density and superconducting pair density, respectively. As for the depletion layer thickness ($x(V_G)$), we assumed the standard functional form of $x(V_G) = x(0)(1 - V_G/V_i)^{1/2}$. By the fitting shown in Fig. 3(a), we obtain W=1.02 μm, R_0=360.8 Ω, $x(0)$=17.8 nm and V_i=0.7 V. The effective width of junction W (1.02 μm) is significantly smaller than the geometrical width of junction W_0 (20 μm), which implies that the supercurrent flows only through narrow paths in the n-InGaAs layer. Using the interfacial resistance (R_0), we define the channel resistance (R_{Ch}) as $R_{\mathrm{Ch}} \equiv R_n - R_0$ and investigate the $I_c R_{\mathrm{Ch}}$ product, which is expected to be proportional to the ratio of carrier densities ($I_c R_{\mathrm{Ch}} = (\hbar/m^*\mu)(n_p/n_q)$) from Eq. (1). The obtained $I_c R_{\mathrm{Ch}}$ product takes a constant value of 10 μV in the gate-controlled region, which confirms our description of new-type JoFET. The estimated value of n_p (3.4×10^{15} cm^{-3}) is comparable to those estimated in other superconductor-based LEDs [4].

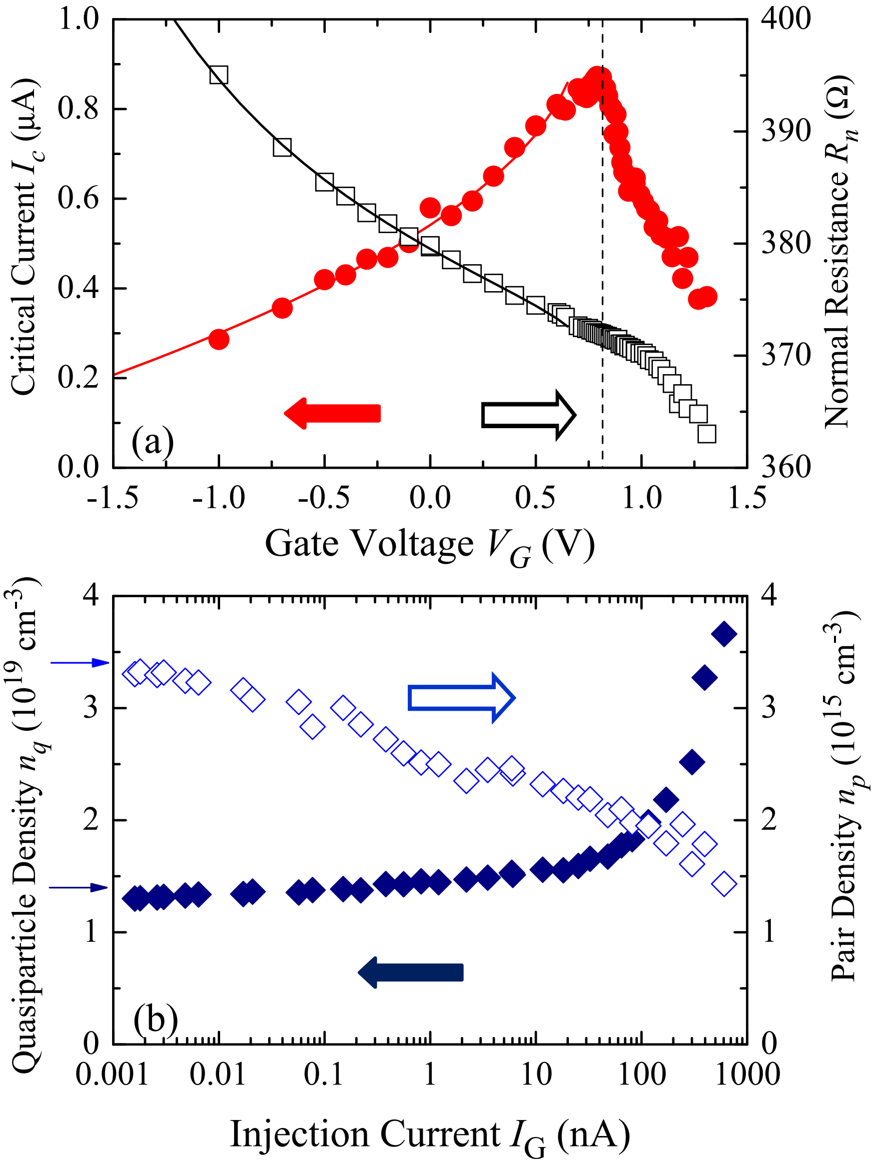

FIG. 3. (a)Superconducting critical current (I_c) and normal resistance (R_n) as functions of gate voltage (V_G). Fitting results in no current injection region is also shown. (b) Estimated quasiparticle density (n_q) and pair density (n_p) in the active layer as functions of injected current (I_G). Arrows in the left vertical axis indicate the values of no injection limit.

When the steady current injection takes place in the current-injected region of $V_G \geq 0.78$ V, both of I_c and R_n decrease with I_G. If we take into account the fact that the depletion layer does not exist in this region ($x(V_G) = 0$) and reconsider Eq. (1), the carrier density in the n-InGaAs active layer (n_q and n_p) are found to be the only variables that can explain the behaviors of R_n and I_c. Figure 3(b) shows n_q and n_p estimated from Eq. (1) as functions of injected current (I_G).

In all the current-injected region, the sum $(n_q + 2n_p)$ increases with I_G. Considering the charge neutrality condition, this increase indicates that the energy of conduction band in the n-InGaAs active layer is pulled down for electrons with respect to vacuum by the current injection. This also means that the energy of valence band is pulled up for holes, which is implied by the tendency of saturation shown in Fig. 2(a).

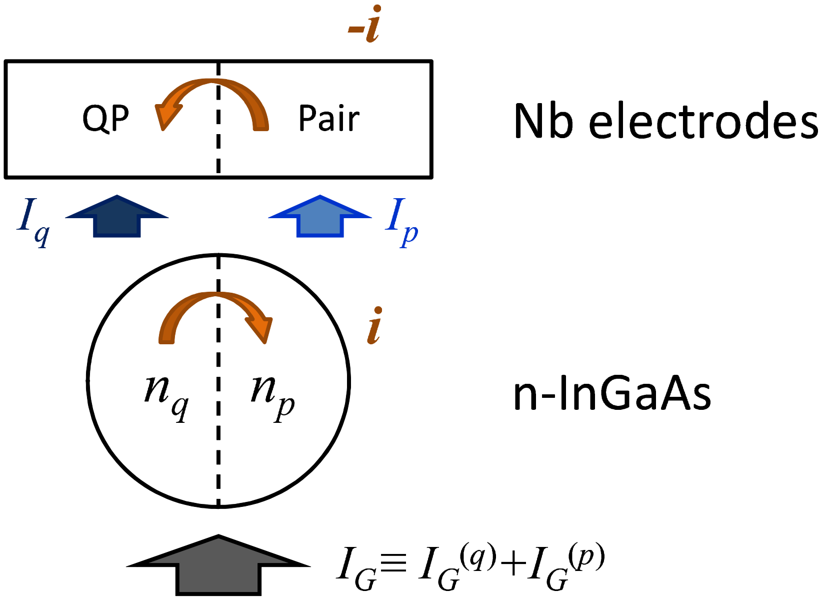

FIG. 4. Schematic diagram of quasiparticles and superconducting pairs.

Next we note that both n_q and n_p do not show the tendency toward saturation in the limit of $I_G \to 0$, the values of which are indicated by arrows in the left vertical axis of Fig. 3(b). In order to explain this high sensitivity for radiative recombination process, we adopt the two-fluid model and consider the flow diagram of quasiparticles and superconducting pairs schematically shown in Fig. 4. Because the total charge conserves in the energy relaxation process in succession to the photon absorption, current with an amount exactly equal to I_G is required to be extracted from the n-InGaAs active layer to the Nb electrodes in the steady state. This means that carriers flow into the conduction band of the n-InGaAs layer to compensate the carrier loss caused by the recombination process. We define I_q and I_p as the current carried by quasiparticles and pairs, and represent the steady state condition as

$$I_q + I_p = I_G \equiv I_G^{(q)} + I_G^{(p)}. \tag{2}$$

Here $I_G^{(q)}$ and $I_G^{(p)}$ are the components of injected hole current (I_G) that recombine with quasiparticles and pairs corresponding to their recombination rates.

In addition to the inflow of carriers (I_q and I_p), the hole current injection causes large disturbance in the quasiparticle - pair system via radiative recombination and the immediate absorption of generated photons, and promotes the conversion from pairs to quasiparticles. If we put the current corresponding to the conversion rate as i, the following condition is also required in the steady state:

$$0 = I_G^{(q)} - I_q - i = I_G^{(p)} - I_p + i. \tag{3}$$

(We define the positive direction of i as the flowing direction from quasiparticle subsystem to pair subsystem taking into account that the charge is negative.)

Generally speaking, the conversion rate from quasiparticles to pairs (i) depends not only on the injected current (I_G) but also on the carrier density (n_q and n_p). However, in the region of $I_G \lesssim 10$ nA, we can assume that the energy relaxation process of absorbed photons dominantly proceeds with the destruction of superconducting pairs and put $i \approx \alpha I_G$. Here the proportional constant α is approximately equal to the ratio of the emitted photon energy to the superconducting pairing energy ($\alpha \approx \hbar\omega_{\mathrm{op}}/\tilde{\Delta}_N$). After solving Eqs. (2) and (3) with respect to I_q and I_p, and taking into account that $\alpha \gg 1$, we obtain

$$\begin{aligned} I_q &= -(\alpha - 1)I_G^{(q)} - \alpha I_G^{(p)} \approx -\alpha I_G, \\ I_p &= \alpha I_G^{(q)} + (\alpha + 1)I_G^{(p)} \approx \alpha I_G. \end{aligned} \tag{4}$$

That is, for compensating the conversion from pairs to quasiparticles inside the n-InGaAs active layer, the superconducting pairs flows *into* the n-InGaAs layer ($I_p > 0$) while the quasiparticles flows *out of* ($I_q < 0$). (To be accurate, the outflow of quasiparticles is a little larger than the inflow of pairs and the steady state condition is secured including the injected hole current.) $|I_q|$ and $|I_p|$ are larger than I_G by the factor of $\alpha \gg 1$, which results in the high sensitivity of Josephson characteristics for monitoring the radiative recombination process.

Here we discuss the effect of heating in the quasiparticle - pair system of the n-InGaAs active layer. If we assume the increase in effective temperature of quasiparticle - pair system of the n-InGaAs layer, the expected flow directions of carriers are opposite to those caused by the conversion described above, which means that the heating works as the damping factor of the compensation cycle. The effect of heating is not dominant in small current injection region of $I_G \lesssim 10$ nA because R_n (and therefore n_q) takes constant value in the temperature range less than 160 mK.

The values of n_q and n_p in steady state are determined as balance points in the carrier flow described in Fig. 4. We can ignore the reformation of superconducting pairs in the n-InGaAs layer because the superconducting pair potential is sufficiently small there. Therefore the superconducting pairs lost in the energy relaxation process are compensated only by the inflow of pairs from Nb superconducting electrodes (I_p), where the discrepancy of chemical potentials in quasiparticle - pair system takes place in order to sustain the reformation rate necessary to the compensation. Due to the large interfacial barriers at Nb electrodes together with the energy shift in the conduction band of n-InGaAs layer, it is difficult to estimate the carrier density in the Nb electrodes ($n_q^{(\mathrm{Nb})}$ and $n_p^{(\mathrm{Nb})}$) directly from those in the n-InGaAs active layer (n_q and n_p). However, we can say that the sudden decrease of n_p in the small current injection region reflects the decrease of $n_p^{(\mathrm{Nb})}$ caused by the rate-limiting reformation.

When the injected current is increased ($I_G \gtrsim 10$ nA), we cannot ignore the recombination process of injected holes with quasiparticles in addition to various energy relaxation processes of absorbed photons other than the destruction of superconducting pairs. Moreover, the effective temperature of quasiparticle / pair subsystem in the n-InGaAs active layer is increased, which causes not only the damping of the compensation cycle but also the suppression of I_c. These effects results in the gradual decrease of the current amplification factor (α), and eventual break down of the flow model described in Fig. 4. Especially in the region of $I_G \gtrsim 0.3$ μA, the transport measurement of Josephson junction characteristics under the steady current injection becomes difficult whereas the spectrally-integrated EL intensity reaches the sensitivity of our optical measurement system as is shown in Fig. 1(c). The injected current (I_G) comparable with the superconducting critical current of the Josephson junction (I_c) causes asymmetric distortion of current - voltage curve which is due to the small difference in the transparency of interface at the two Nb electrodes.

In conclusion, we quantitatively studied the transport properties of Josephson junction attached to superconductor-based LED. In the gate-controlled region, we confirm the realization of new-type Josephson field effect transistor (JoFET), where the channel cross-sectional area of the junction is directly modulated. In the current-injected region, the energy relaxation process of generated photons in succession to the radiative recombination process causes the conversion of superconducting pairs to quasiparticles in the active layer, and the carrier flows for compensating the conversion.

We appreciate Dr. S. Kim for fruitful discussion.

---

* ryoinoue@crm.rcast.u-tokyo.ac.jp

[1] Y. Asano, I. Suemune, H. Takayanagi and E. Hanamura, Phys. Rev. Lett. **103**, 187001 (2009).

[2] P. Recher, Y. V. Nazarov and L. P. Kouwenhoven, Phys. Rev. Lett. **104**, 156802 (2010).

[3] Y. Hayashi, K. Tanaka, T. Akazaki, M. Jo, H. Kumano and I. Suemune, Appl. Phys. Express **1** 011701 (2008).

[4] I. Suemune, Y. Hayashi, S. Kuramitsu, K. Tanaka, T. Akazaki, H. Sasakura, R. Inoue, H. Takayanagi, Y. Asano, E. Hanamura, S. Odashima and H. Kumano, Appl. Phys. Express **3** 054001 (2010).

[5] H. Sasakura, S. Kuramitsu, Y. Hayashi, K. Tanaka, T. Akazaki, E. Hanamura, R. Inoue, H. Takayanagi, Y. Asano, C. Hermannstädter, H. Kumano and I. Suemune, Phys. Rev. Lett. **107**, 157403 (2011).

[6] R. Inoue, H. Takayanagi, T. Akazaki, K. Tanaka and I. Suemune, Supercond. Sci. Tech. **10**, 034025 (2010).

[7] T. Akazaki, H. Takayanagi, J. Nitta and T. Enoki, Appl. Phys. Lett. **68**, 418 (1996).

[8] T. Schäpers, J. Malindretos, K. Neurohr, S. G. Lachenmann, A. van der Hart, G. Crecelius, H. Hardtdegen, H. Lüth, M. Behet and A. A. Gollubov, Appl. Phys. Lett. **73**, 2348 (1998).

[9] J. J. A. Baselmans, A. F. Morpurgo, B. J. van Wees and T. M. Klapwijk, Nature **397**, 43 (1999).

[10] D. Beckmann, H. B. Weber, and H. v. Lhneysen, Phys. Rev. Lett. **93**, 197003 (2004).

[11] S. Russo, M. Kroug, T. M. Klapwijk, and A. F. Morpurgo, Phys. Rev. Lett. **95**, 027002 (2005).